Journal of Engineering Physics and Thermophysics, Vol. 76, No. 2, 2003

NUMERICAL ANALYSIS OF THE JET-VORTEX PATTERN OF FLOW IN A RECTANGULAR TRENCH

S. A. Isaev,[a] **P. I. Kudinov,**[b]
N. A. Kudryavtsev,[a] **and I. A. Pyshnyi**[a]

UDC 532.517.2

Numerical simulation of the vortex structure of three-dimensional laminar flow in a rectangular trench of square cross section has been carried out on the basis of the finite-volume solution of steady-state Navier–Stokes equations.

Introduction. Identification of three-dimensional jet-vortex structures in developed separated flows represents one of the topical problems of modern hydromechanics. Currently a numerical analysis has been made of a totality of various three-dimensional problems of vortex dynamics: circulatory fluid flow in a cubic cavity with a mobile cover [1], turbulent flow in a rectangular channel with a circular cavity located on one of its walls [2], laminar flow (past a cylinder with a coaxial front disk at the angle of attack [3, 4], and laminar [5–7] and turbulent [8–10] near-wall flows in the neighborhood of holes having different shapes. It has been revealed that the flow-forming elements of large-scale vortex structures in the three-dimensional separation zones have a topology of the same type. The influence of the Reynolds number on their dynamics is understood to a certain degree.

It should be noted that the regularities in the behavior of three-dimensional flows can differ radically from the well-studied dependences for their two-dimensional analogs. In particular, this can be due to the stability loss by the plane-parallel fluid motion. Moreover, for the same geometric configurations there can exist several structures of flow, some of which (two-dimensional or possessing symmetry, as a rule) can be unstable and capable, on introduction of disturbances, of transforming into more stable three-dimensional configurations [11, 12].

It should also be emphasized that the possibilities of experimental investigations of vortex dynamics are limited in many respects, since it is difficult to perform a detailed visualization of the entire structure of three-dimensional flow. The methods of soot-oil coatings are most informative [13], but they give an idea of only the lines of spreading of the fluid on solid surfaces. They are insufficiently informative for an understanding of the volume structure of flow, especially in the case of unstable nonstationary flows. Therefore, one prefers numerical methods for investigating the three-dimensional structures of flow.

The three-dimensional character of flow presents a specific problem for numerical simulation, since large arrays of numerical data should be interpreted graphically in this case. For interpretation of three-dimensional vortex dynamics one most successfully uses the following methods: tracking the trajectories of individual particles, visualization of different isosurfaces (for example, the surfaces of stream, isotachs, stresses, and temperatures), and analysis of the distributions of parameters in the selected plane-parallel cross sections. Three-dimensional vortex flow can be considered as a set of solutions of the type of a strange attractor. Each attractor represents in fact a large-scale structure of flow. The most widespread configurations in motion of a liquid medium near solid boundaries are tornado-like and toroidal vortices. Moreover, complex large structures every so often consist of smaller structures; therefore, to obtain an idea of the entire structure of flow it is sometimes necessary to view as many as several hundred trajectories to finally select the most informative ten of them.

In the present work, we continue the numerical investigation (started in [1]) of the jet-vortex structures induced in an elongated rectangular trench of square cross section by the motion of one of its extended boundaries with a constant velocity. The aim of the investigation is also methodological analysis of the computational algorithms for simulation of three-dimensional separated flows. In this investigation, as in the recent publication [1], prominence is

[a]Academy of Civil Aviation, St. Petersburg, Russia; email: isaev@SI3612.spb.edu; [b]Dnepropetrovsk State University, Dnepropetrovsk, Russia. Translated from Inzhenerno-Fizicheskii Zhurnal, Vol. 76, No. 2, pp. 24–30, March–April, 2003. Original article submitted August 28, 2002.

1062-0125/03/7602-0257$25.00

given to the mechanism of fluid spreading of the fluid on the trench walls. We used the TECPLOT 7.5 package that provides vast possibilities for computer visualization of flows.

Computational Methodology. Various problems of flow of an incompressible fluid are most frequently solved by SIMPLE-type methods [14]. Variants of generalization of these methods to the case of a curvilinear coordinate system are discussed in a number of works [14–17]. The method developed in [14, 15] makes it possible to carry out calculations on nonorthogonal grids; however, only the SIMPLE or SIMPLEC (coordinated variant of SIMPLE) methods can be used in calculations on partially or completely matched grids. In [18], the SIMPLER method has been formulated for the case of orthogonal curvilinear coordinates.

In the present work, we have generalized a set of SIMPLE algorithms to the case of an arbitrary curvilinear coordinate system on a spaced staggered grid. Owing to the form of representation proposed, the discrete analogs of the initial equations are completely coincident in form with the equations used for derivation of the base SIMPLE, SIMPLEC, SIMPLER, and PISO procedures on a spaced Cartesian grid. Therefore, unlike approaches of the type of the Rhie–Chow method [19], any SIMPLE-type algorithm can be implemented within the framework of the generalization proposed. A peculiarity of the approach proposed is that the discrete analogs of the equations and the numerical solutions obtained on the Cartesian grid identically coincide with those obtained with the use of the corresponding base SIMPLE algorithm written for the Cartesian coordinate system.

As the initial equations, we take the Navier–Stokes equations written as conservation laws in integral vector form:

$$\oiint_S (\mathbf{V}\mathbf{n}\,\rho)\, dS = 0\,, \tag{1}$$

$$\iiint_W \frac{\partial \rho \mathbf{V}}{\partial t}\, dW + \oiint_S \left[\mathbf{V}\mathbf{n}\,(\rho\mathbf{V}) - \mu\left(\frac{\partial \mathbf{V}}{\partial n}\right)\right] dS = -\iiint_W \nabla p\, dW + \iiint_W \mathbf{G}\, dW\,. \tag{2}$$

To implement the universal numerical method, we can conveniently write Eqs. (1) and (2) in the form of the generalized law of conservation of the physical quantity Φ in the control volume:

$$\iiint_W \frac{\partial \rho \Phi}{\partial t}\, dW + \oiint_S \left[\mathbf{V}\mathbf{n}\,(\rho\Phi) - \Gamma\left(\frac{\partial \Phi}{\partial n}\right)\right] dS = \iiint_W S_\Phi\, dW\,. \tag{3}$$

The discrete analog of (3) will have the form

$$A_0\Phi_0 = -\sum_k A_k\Phi_k + S_\Phi \Delta W + S'_\Phi + \frac{\rho \Delta W}{\Delta t}\,\Phi_0^{n-1}\,, \tag{4}$$

$$A_0 = -\sum_k A_k + \frac{\rho \Delta W}{\Delta t}\,, \tag{5}$$

$$S'_\Phi = -\Phi_0 \sum_k \left[(-1)^k V^j \rho\right] \Delta S_k / |\mathbf{e}^i| + \sum_k d_k \Gamma \left((-1)^k g^{ij} \Delta_j \Phi\right)_k \Delta S_k / |\mathbf{e}^i|\,, \tag{6}$$

where Φ_0^{n-1} is the value of the variable on the previous time layer;

$$A_k = \sum_k \left[(-1)^k V^j \rho c_k - d_k \Gamma \left(g^{ii} \frac{1}{\Delta x_k}\right)_k\right] \Delta S_k / |\mathbf{e}^i|\,, \quad k = 2i-1\,,\ \ 2i\,,\ \ i = 1, 2, 3\,. \tag{7}$$

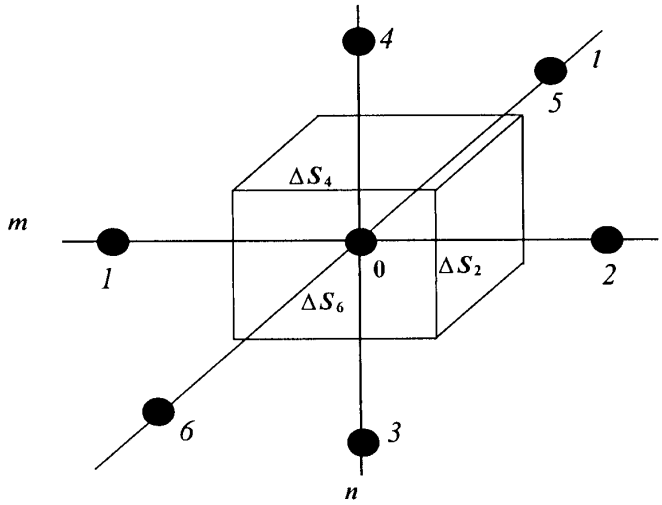

Fig. 1. Numbering of the points of the space grid.

The numbering of the points and faces of the control volume is carried out in the following way: the point at the center is assigned the number 0, the point shifted relative to the zero point by a step in the forward direction along the ith coordinate is assigned the number $k = 2i$, the point shifted by a step in the backward direction is assigned the number $k = 2i - 1$, and the face lying between the zero and kth points is assigned the number k. Thus, if a regular grid is introduced in the three-dimensional region, the point (l, m, n) corresponds to the local point 0 and the local numbers of the neighboring points are $(l-1, m, n) = 1$, $(l+1, m, n) = 2$, $(l, m-1, n) = 3$, $(l, m+1, n) = 4$, $(l, m, n-1) = 5$, and $(l, m+1, n+1) = 6$ (Fig. 1).

All the results have been obtained by calculation based on the control-volume method and on the generalization of the class of algorithms of the SIMPLE and SIMPLER type for the case of a spaced curvilinear nonorthogonal grid.

To increase the accuracy, we used an ISNAS monotone TVD scheme of third order of accuracy. The value of the function on the face of the control volume has the form

$$(\Phi)_k = (\Phi_{\mathrm{UDS}})_k + \Psi_k \,. \tag{8}$$

For the ISNAS TVD scheme of third order of accuracy [20] the limiter Ψ_k on a uniform grid has the form

$$\Psi_k = \begin{cases} \dfrac{1}{2}\Delta\Phi_0 \dfrac{(\Delta\Phi_1^2 + 3\Delta\Phi_0\Delta\Phi_1)}{(\Delta\Phi_0 + \Delta\Phi_1)^2}, & \Delta\Phi_1\Delta\Phi_0 > 0\,, \\ 0\,, & \Delta\Phi_1\Delta\Phi_0 \le 0\,, \end{cases} \tag{9}$$

where

$$\Delta\Phi_0 = \begin{cases} (\Phi_k - \Phi_0)\,, & (\mathbf{Vn})_k \ge 0\,, \\ (\Phi_0 - \Phi_k)\,, & (\mathbf{Vn})_k < 0\,; \end{cases} \qquad \Delta\Phi_1 = \begin{cases} (\Phi_0 - \Phi_{-k})\,, & (\mathbf{Vn})_k \ge 0\,, \\ (\Phi_k - \Phi_{+k})\,, & (\mathbf{Vn})_k < 0\,. \end{cases}$$

The condition $\Delta\Phi_1\Delta\Phi_0 < 0$ corresponds to the case where a local extremum is positioned upstream of the kth face. As follows from (9), here $(\Phi)_k$ is calculated in fact by the upwind difference scheme, which, however, does not lead to a decrease in the order of approximation [20] and provides the conditions under which the local extremum does not increase.

For comparison with the above-described algorithm, in the present work we also use the computational algorithm based on the concept of splitting by physical processes and the use of consistent structurized grids [14, 15]. This

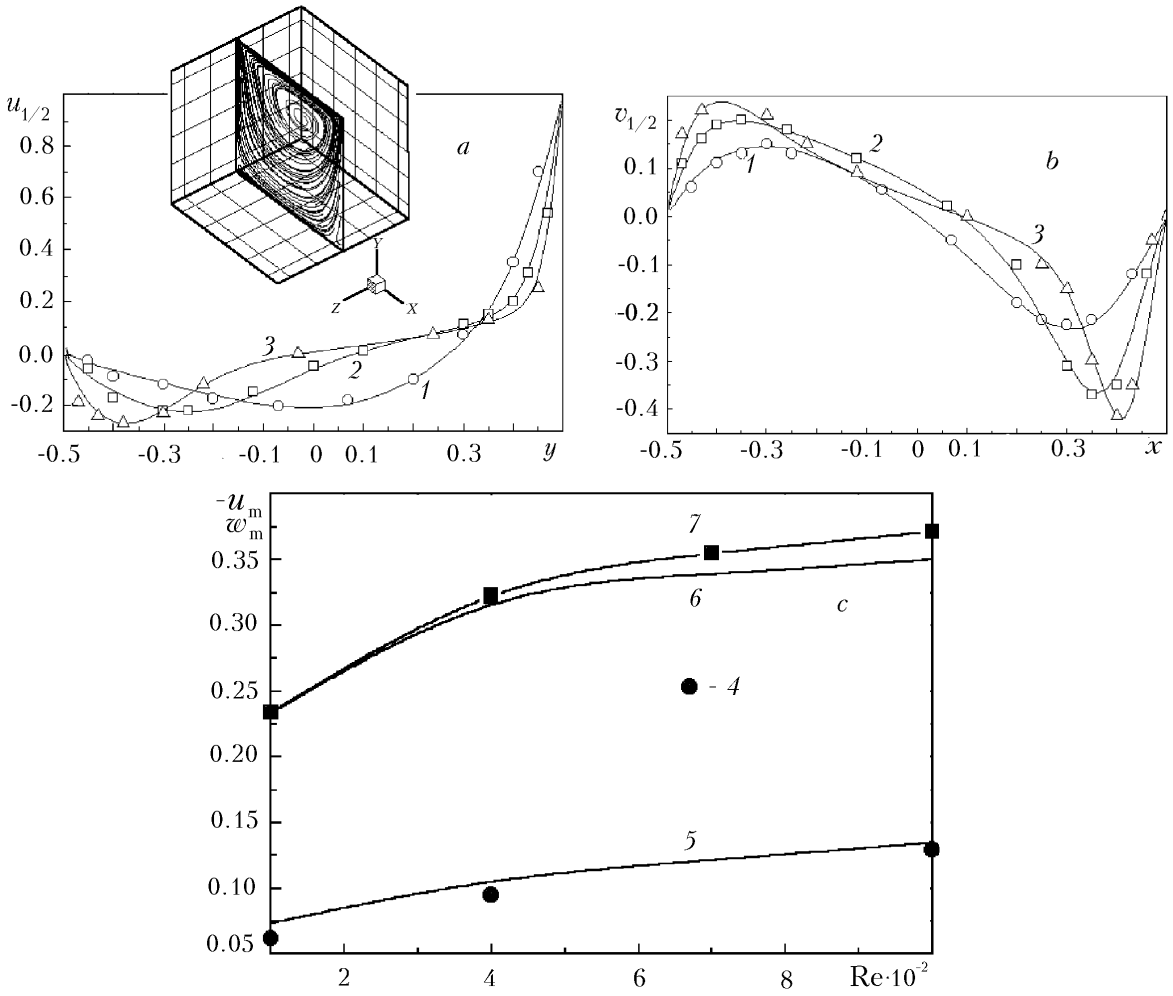

Fig. 2. Comparison of the calculated profiles of the horizontal (a) and vertical (b) velocity components in the middle cross section of the cubic cavity at different Re numbers and of the dependences of the maximum values of the transverse and longitudinal velocity components in the rectangular cavity on the Reynolds number (c); the points in a and b are taken from [21]; 1) Re = 10^2, 2) $4 \cdot 10^2$, 3) 10^3, 4) this work, and 5) [1, 15]; 6, 7) calculations by the method of [1, 15] for the three-dimensional and two-dimensional cavities.

algorithm is realized in the process of global interaction, whose constituent part is the known SIMPLEC procedure of pressure correction. This two-step procedure of the "predictor–corrector" type is meant for determining the Cartesian components of the velocity and the pressure.

The original features of the finite-volume algorithm are associated with (a) representation of the initial equations in increments of dependent variables, (b) approximation of the convective terms on the explicit side by Leonard's upwind scheme with quadratic interpolation, (c) approximation of the convective terms on the implicit side by the upwind scheme with one-sided differences, (d) introduction of artificial diffusion into the implicit side for damping of the high-frequency oscillations, (e) use of the Rhie–Chow monotonizer in the block of pressure correction because of the centered computational template with an empirically determined coefficient of 0.1, and (f) solution of the difference equations by the method of incomplete matrix factorization.

Testing. Stationary circulatory flow of an incompressible viscous fluid in cubic and rectangular cavities with a mobile face [1] is considered as the model problem for testing the algorithms developed. The characteristic quantities selected for solving the problem are the length of the edge of square cross section and the velocity of motion of the upper cover. The calculations were carried out with grids concentrated near the boundaries and containing

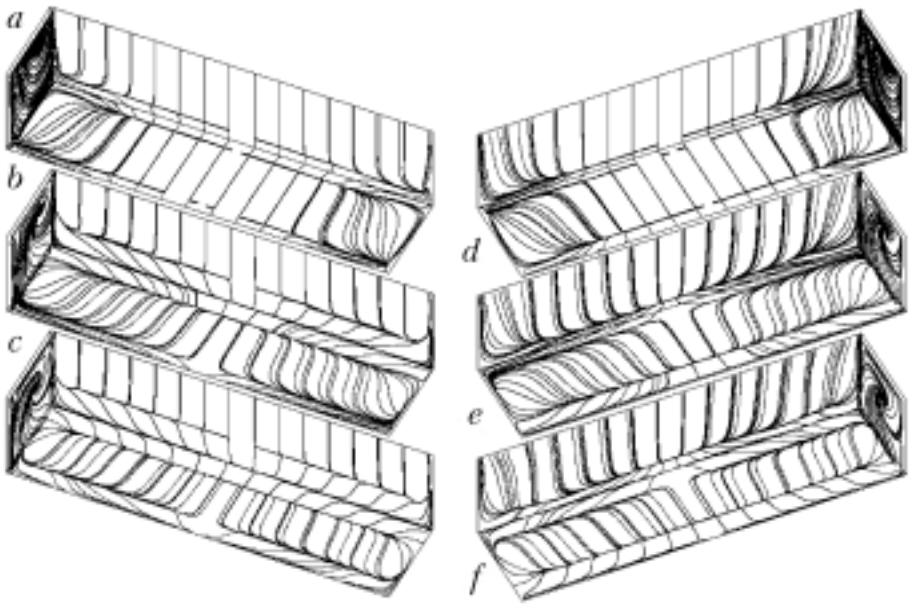

Fig. 3. Patterns of spreading of the fluid on the bottom, side, and back (downstream) faces of the rectangular cavity: a, d) Re = 10^2; b, e) $4 \cdot 10^2$; c, f) 10^3.

$40 \times 40 \times 40$ cells for the cubic cavity and $40 \times 40 \times 70$ cells for the rectangular cavity with an elongation of 4. The minimum step near the walls was selected to be 0.005. The Reynolds number varied from 10^2 to 10^3.

A comparative analysis of the profiles of the horizontal and vertical velocity components in the middle cross section of the cubic cavity, presented in Fig. 2a and b, shows that the data of calculations by the above-described method on the spaced grid are in good agreement with the analogous data [21] obtained on the consistent grid with the same arrangement of the grid points. It should be noted that the calculation data obtained in [1, 21] also agree with an acceptable accuracy.

Figure 2c shows a comparison of the dependences of the maximum values of the transverse velocity component in the rectangular trench on the Reynolds number which have been obtained by the method proposed and within the framework of the approach of [1, 15]. It has been revealed that there is a certain disagreement between the results at low and moderate Re, although the accuracy of the predictions seems quite acceptable. It should be noted that the comparative analysis performed earlier in [22] of the results of the calculation of circulatory two-dimensional flows in a square cavity on staggered and consistent grids has shown that the first approach has an advantage for accuracy. This conclusion was not confirmed by the data obtained in the present work as a result of simulation of three-dimensional flow in a cubic cavity. On the contrary, it has been shown that the predictions made with different types of grids have the same accuracy when computational algorithms close in order of approximation are used.

Analysis of the Results. Some of the results obtained are shown in Figs. 2–6. First and foremost, it is of interest to compare the dependences of the maximum longitudinal component of the velocity of a circulatory flow in the elongated trench and in the square cavity on the Reynolds number when it changes from 10^2 to 10^3 (Fig. 2c). The small difference between them points to a fairly weak (but progressing with increase in Re) decelerating action of the side walls on the flow of a viscous fluid in the central part of the trench. This conclusion conforms with the analogous conclusion drawn in [2] for turbulent flow in the circular cavity located on the wall of a plane-parallel channel having a much smaller elongation of the trench (of the order of one and a half of the cavity diameter).

In Fig. 3, the patterns of spreading of the flow on the walls of the rectangular trench at different values of the Reynolds number are compared. As has been noted in [1] for the cubic cavity, on all the faces of the trench there are singular points of the type of a focus and the lines of sink flow and spreading of the fluid. Thus, at the bottom of the cubic cavity, the evolution of the pattern of spreading with increase in the Reynolds number from Re = 10^2 was accompanied by a decrease in the influence of the side walls and transformation of the sink flow to the line of sink flow at Re = 10^3. The indicated sink flow was formed in the process of attachment of the separated flow in the central part of the cavity to its bottom face.

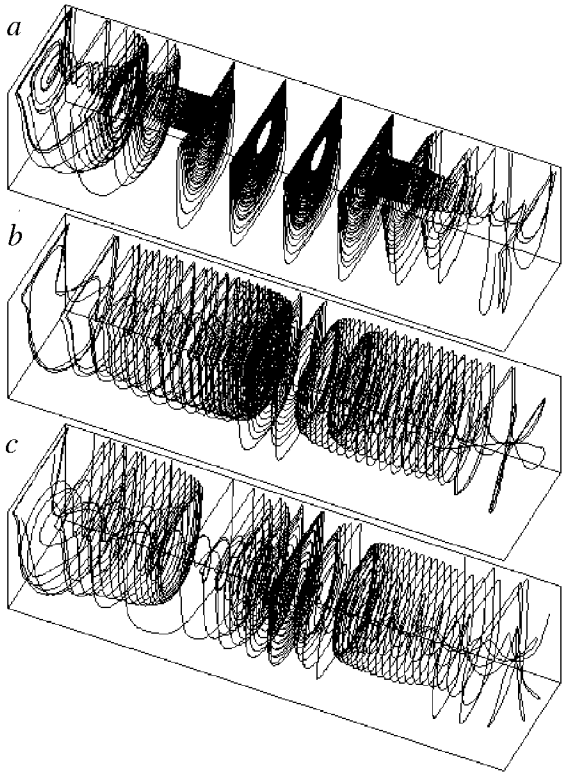

Fig. 4. Vortex structures in the rectangular cavity: a) Re = 10^2; b) $4 \cdot 10^2$; c) 10^3.

Such a sink flow is not formed at the bottom of a rectangular trench since the separated flow on the back extended wall of the cavity causes the formation of a continuous line of sink flow. As Re increases, the dimensions of the separation zone in the corner neighborhood of the bottom and the back wall increase markedly.

Approaching the front wall, the fluid forms the line of spreading and separates; just as the line of sink flow, this line is virtually parallel to the front wall. In the central part of the trench, the streamline at the bottom is parallel to the side walls and the fluid motion is quasi-two-dimensional in character.

The vortex dynamics in the neighborhood of the side walls and the bottom of the trench was found to be the same as for the cubic cavity.

The interaction of the flows spreading on the bottom of the cavity occurs along the line of spreading of the fluid near the front wall. It is significant that this interaction results in the formation of two symmetric peripheral sources. As follows from the analysis of such vortex formations in the case of flow in the front separation zone localized in the gap between the disk and the face of the cylinder [3, 4], the fluid from the indicated sources goes from the wall in the form of swirling jets. As the Reynolds number increases, these sources move to the neighborhood of the edges of the side faces.

Judging from the directions of the streamlines at the bottom of the trench, the fluid motion in the neighborhood of the front wall is directed from the central part of the trench to the side walls.

Fluid flow on the front (upstream) face is determined on the whole by the carrying action of the mobile wall. As in the case of a cubic cavity [1], in the neighborhood of the mobile wall the streamlines are virtually parallel to each other, but they are markedly twisted near the bottom, especially at moderate and high Re.

Fluid motion on the back (downstream) wall is caused by the interaction of this wall with the shear flow formed as a result of the motion of the upper cover with a constant velocity. Therefore, the streamlines directed to the bottom of the trench are virtually parallel to the side walls on the major part of the face considered. However, in the vicinity of the side walls, as in the case of a cubic cavity, there arise sources induced by the flow of fluid from the central part of the trench to the periphery. It should be noted that they move from the bottom as the Reynolds number increases.

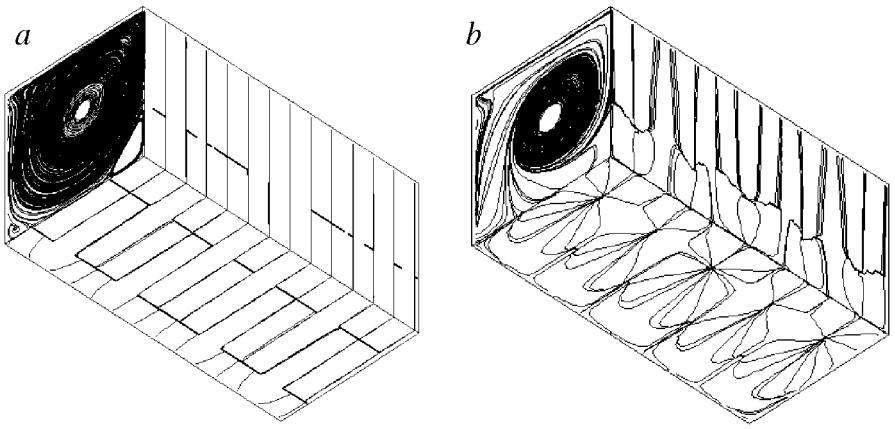

Fig. 5. Patterns of flow in the cross sections of the unbounded cavity at Re = 10^3 (a) and $1.5 \cdot 10^3$ (b).

On each of the side walls of the cavity, there arises swirling fluid motion with a source localized in the central part; a portion of the fluid from the corner separation zones is involved in it. As the Reynolds number increases, the source moves to the geometric center of the side face.

The dynamics of the three-dimensional jet-vortex structures with increase in the Reynolds number is analyzed in Fig. 4. The distinctive features of the hydrodynamic elements formed in the trench coincide with the analogous features for the cubic cavity [1]. Introduction of a particle in the neighborhood of the source on the side wall reveals the formation of a swirling jet flow directed to the central part of the trench. However, unlike the cubic cavity for which the indicated jet flows moving from the side walls interact in the central plane even at low (of the order of 10^2) Reynolds numbers, there is no such collision of the jets in the elongated trench. At Re = 10^2, their intensity determined by the transverse pressure drop is obviously insufficient to transport the fluid to large distances from the side walls. Therefore, the flow circulating in the trench can be separated into quasi-two-dimensional reverse-circulatory flow in the central part (the same in the longitudinal sections) and complex fluid motion in the peripheral zones adjacent to the side walls.

The tracks of the particles introduced in the corner neighborhood of the bottom and the front wall show an unusual kind of dynamics of the fluid in the trench: its flow on the side wall to the source, tornado-like movement of the particles to the central plane, and spinning of the particles followed by their drift in the peripheral layers in the direction to the side wall.

Fluid motion in a trench, as in a cubic cavity, is on the whole analogous to that in a vortex tube. It should be noted that the behavior of a vortex flow has identical features in different types of problems: external separated flow past a cylinder with a forward coaxial disk [3, 4], flow around an isolated deep hole on the plane [5–10], and fluid motion in a plane-parallel channel with a circular vortex cell on one of the walls [2], in a cubic cavity [1], and in the three-dimensional vortex flow in the trench considered.

As the Reynolds number increases, the separated flow in the trench is intensified, cross transfer is enhanced, and the carrying of swirling jets from the side walls increases.

It should be noted that the results of our investigation correlate quite satisfactorily with the data of the numerical analysis of the structure of the flow circulating in the trench with an elongation of 3 which has been carried out in the nonstationary formulation in a wide range of Reynolds numbers (1–3200) [23]. Unfortunately, the use of fairly coarse computational grids in longitudinal sections of the cavity (34×34) prevents the indicated data from being considered as acceptable in accuracy at high Reynolds numbers. Nonetheless, the stability loss by the three-dimensional separated flow at high Reynolds numbers and the wave character of fluid motion in the cavity are also distinctive features of the considered type of flow which were borne out by experiment.

In the methodological aspect, it is of interest to analyze flow in a trench of infinite elongation, i.e., without taking into account the influence of the side walls. The results presented do undescore a very strong influence of the side walls of the trench on the formation of the secondary cross flow, which progresses with increase in Re. There-

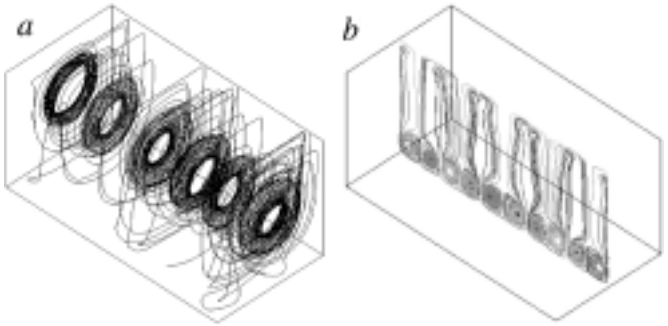

Fig. 6. Vortex structures in the unbounded cavity (a) and trajectories of particles in the longitudinal and cross sections, obtained as a result of the nulling of the longitudinal velocity component (b). Re = $1.5 \cdot 10^3$.

fore, it seems reasonable to consider separated flow in an isolated module of an infinite cavity of square cross section with the setting of slipping conditions at the side boundaries.

In Fig. 5, the patterns of spreading of fluid in longitudinal sections and on the walls of the cavity at Reynolds numbers of 10^3 and $1.5 \cdot 10^3$ are compared. A distinguishing characteristic of three-dimensional separated flow is its separation into cells. It should be noted that the tendency toward forming such a structure of flow has been underscored in [11], where the fluid spreading on the walls of a cubic cavity at Re = $2 \cdot 10^3$ was analyzed.

If at Re = 10^3 flow in the longitudinal section of an infinite cavity is analogous to circulatory flow in the middle cross section of an elongated trench, at Re = $1.5 \cdot 10^3$ they significantly differ from each other.

The separation of the circulatory flow into vortex cells is illustrated in Fig. 6. In the central part of the cavity, there arise periodic vortex rings revealed in structural analysis of flow in the cubic cavity at Re = 10^2. The vortex ring formed by a fluid particle determines the space zone of the blocked flow much as the vortex rings are formed in deep holes on the plane [5–10]. Their formation is an integral part of virtually all the three-dimensional separated flows.

Noteworthy is the secondary descending of the fluid in the middle cross section of the cavity, which ends within the limits of the isolated vortex cell as pair spiral-like vortex structures (Fig. 6b).

This work was carried out with financial support from the Russian Foundation for Basic Research, project Nos. 02-02-17562, 02-02-81035, and 02-01-01160.

NOTATION

t, time; x, y, z, Cartesian coordinates; u, v, w, Cartesian components of the velocity; W, control volume; S, surface of W; $\mathbf{n}$, outer normal to S; $\mathbf{V}$, velocity vector; ρ, density (it is assumed to be constant in the case of an incompressible fluid); p, pressure; μ, coefficient of viscosity; $\mathbf{G}$, vector of mass forces; Γ, diffusion coefficient; S_Φ, power of the sources Φ; V^i, contravariant components of the velocity vector; $k = 2i - 1$ and $2i$, $i = 1$, 2, and 3; $\mathbf{e}^i$ and $\mathbf{e}^j$, ith covariant and jth contravariant vectors of the local basis; d_k, scheme coefficient; $g^{ij} = \mathbf{e}^i\mathbf{e}^j$, components of the metric tensor; $(\Delta j\Phi)_k$, finite-difference approximation of the derivatives along the kth face of the control volume; $(\Phi_{UDS})_k$, value of the function on the face of the control volume calculated by the upwind difference scheme (UDS); Ψ_k, nonlinear limiter of flows that is a function of the arbitrary parameter Φ in the neighborhood of the kth face of the control volume; Re, Reynolds number. Subscripts: 1/2, parameters in the middle cross section of the cubic cavity; m, maximum values; Φ, physical quantity.

REFERENCES

1. S. A. Isaev, A. G. Sudakov, N. N. Luchko, et al., *Inzh.-Fiz. Zh.*, **75**, No. 1, 49–53 (2002).
2. P. A. Baranov, S. V. Guvernyuk, M. A. Zubin, et al., *Izv. Ross. Akad. Nauk, Mekh. Zhidk. Gaza*, No. 5, 44–56 (2000).
3. S. V. Guvernyuk, S. A. Isaev, and A. G. Sudakov, *Zh. Tekh. Fiz.*, No. 11, 138–142 (1998).

4. V. K. Bobyshev, S. V. Guvernyuk, and S. A. Isaev, *Inzh.-Fiz. Zh.*, **72**, No. 4, 634–640 (1999).
5. S. A. Isaev, A. I. Leont'ev, D. P. Frolov, et al., *Pis'ma Zh. Tekh. Fiz.*, **24**, Issue 6, 6–12 (1998).
6. S. A. Isaev, A. I. Leont'ev, A. E. Usachov, et al., *Izv. Ross. Akad. Nauk, Énergetika*, No. 2, 126–136 (1999).
7. S. A. Isaev, A. I. Leont'ev, P. A. Baranov, et al., *Inzh.-Fiz. Zh.*, **74**, No. 2, 62–67 (2001).
8. S. A. Isaev, A. I. Leont'ev, and P. A. Baranov, *Pis'ma Zh. Tekh. Fiz.*, **26**, Issue 1, 28–35 (2000).
9. S. A. Isaev, A. I. Leont'ev, P. A. Baranov, et al., *Dokl. Ross. Akad. Nauk*, **373**, No. 5, 615–617 (2000).
10. S. A. Isaev, A. I. Leont'ev, and Kh. T. Metov, *Inzh.-Fiz. Zh.*, **75**, No. 4, 98–101 (2002).
11. P. I. Kudinov, Physical Principles of Experimental and Mathematical Modeling of Processes of Gas Dynamics and Heat Transfer in Power Plants, in: *Proc. XIII School-Seminar of Young Scientists and Specialists guided by Academician A. I. Leont'ev* [in Russian], Vol. 1, Moscow (2001), pp. 149–152.
12. F. Durst, J. C. F. Pereira, and C. Troperea, *J. Fluid Mech.*, **248**, 567–581 (1993).
13. V. I. Terekhov, N. I. Yarygina, A. Yu. D'yachenko, et al., in: *Proc. IV Minsk Int. Forum "Heat and Mass Transfer–MIF-2000"* [in Russian], 22–26 May 2000, Minsk, Vol. 1, Minsk (2000), pp. 28–35.
14. I. A. Belov, S. A. Isaev, and V. A. Korobkov, *Problems and Methods of Calculation of Separated Flows of an Incompressible Fluid* [in Russian], Leningrad (1989).
15. S. A. Isaev, P. A. Baranov, N. N. Luchko, et al., *Numerical Modeling of Separated Flow of an Incompressible Fluid in Square and Cubic Cavities with a Moving Boundary* [in Russian], Preprint No. 7 of A. V. Luikov Heat and Mass Transfer Institute, National Academy of Sciences of Belarus, Minsk (1999).
16. Y. S. Chen, A Numerical Method for Three-Dimensional Incompressible Flow Calculations Using Nonorthogonal Body-Fitted Coordinate Systems, *AIAA Paper*, No. 86–1654 (1986).
17. C. R. Maliska and G. D. Rathby, *Int. J. Numer. Meth. Fluids*, **4**, No. 6, 87–95 (1984).
18. S. Ya. Grabarnik and D. S. Tsepov, *Matem. Modelir.*, **10**, No. 10, 103–111 (1998).
19. S. M. Rhie and W. L. Chow, *Aérokosm. Tekh.*, **2**, No. 7, 33–43 (1984).
20. M. Zijlema, *On the Construction of Third-Order Accurate TVD Scheme Using Leonard's Normalized Variable Diagram with Application to Turbulent Flows in General Domains*, Technical Report DUT-TWI-94-104, Delft University of Technology (1994).
21. V. I. Pokhilko, *Solution of the Navier–Stokes Equations in a Cubic Cavity* [in Russian], Preprint No. 11 of the Institute of Mathematical Modeling of the Russian Academy of Sciences, Moscow (1994).
22. S. A. Isaev and A. E. Usachov, *Prom. Aérodinam.*, Issue 4 (36), 43–75 (1991).
23. T. P. Chiang, W. H. Sheu, and R. R. Hwang, *Int. J. Numer. Meth. Fluids*, **26**, No. 5, 557–579 (1998).